Published in final edited form as:
Dev Cell. 2012 August 14; 23(2): 397–411. doi:10.1016/j.devcel.2012.06.014.

The Microtubule-associated Rho Activating Factor GEF-H1 interacts with Exocyst complex to regulate Vesicle Traffic

Ritu Pathak[1], **Violaine D. Delorme-Walker**[1], **Michael C. Howell**[1], **Anthony N. Anselmo**[1], **Michael A. White**[3], **Gary M. Bokoch**[1,2,*], and **Céline DerMardirossian**[1,4,*]

[1]Departments of Immunology and Microbial Science and [2]Cell Biology, The Scripps Research Institute, 10550 N. Torrey Pines Road, La Jolla, CA 92037, USA [3]Department of Cell Biology, University of Texas Southwestern Medical Center, 5323 Harry Hines Blvd., Dallas, TX 75220-9039, USA

SUMMARY

The exocyst complex plays a critical role in targeting and tethering vesicles to specific sites of the plasma membrane. These events are crucial for polarized delivery of membrane components to the cell surface, which is critical for cell motility and division. Though Rho GTPases are involved in regulating actin dynamics and membrane trafficking, their role in exocyst-mediated vesicle targeting is not very clear. Herein, we present evidence that depletion of GEF-H1, a guanine nucleotide exchange factor for Rho proteins, affects vesicle trafficking. Interestingly, we found that GEF-H1 directly binds to exocyst component Sec5 in a Ral GTPase-dependent manner. This interaction promotes RhoA activation, which then regulates exocyst assembly/localization and exocytosis. Taken together, our work defines a mechanism for RhoA activation in response to RalA-Sec5 signaling and involvement of GEF-H1/RhoA pathway in the regulation of vesicle trafficking.

INTRODUCTION

Membrane trafficking is crucial for delivery of specific membrane and protein components to defined sites on the cell surface during cell division, migration, and secretion (Caswell and Norman, 2008; Montagnac et al., 2008). The polarized membrane delivery in many cell types is regulated by an evolutionarily conserved protein complex, termed “exocyst” which comprises eight proteins, Sec3, 5, 6, 8, 10, 15 and Exo70, 84. The exocyst is a dynamic complex assembled from subunits that form a targeting patch on the plasma membrane (PM) and a vesicle-associated sub-complex, which function together to both target and tether vesicles to specific sites of the dynamic PM (He and Guo, 2009). The exocyst plays important roles in targeting membrane to the expanding leading edge, as well as adhesion and signaling molecules necessary for motility and chemotaxis. Exocyst components are also involved in several endocytic pathways in polarized MDCK cells (Oztan et al., 2007). Furthermore, exocyst proteins interact with the recycling endosomes as well as exocytic

[4]To whom correspondence should be addressed at dmceline@scripps.edu, phone: 858-784-8217, Fax: 858-784-8218.
*These authors contributed equally to this work

vesicles to regulate their tethering at the cleavage furrow to drive abscission during cytokinesis (Fielding et al., 2005; Gromley et al., 2005).

Small GTPases of the Rab, Arf and Ral families have been implicated as important spatio-temporal regulators of membrane trafficking events by the exocyst (Novick and Guo, 2002; Prigent et al., 2003). Studies done in yeast implicate Rho GTPases also in regulation of exocyst function (Guo et al., 2001). However, the role of mammalian Rho GTPases in exocyst-mediated vesicle targeting is not very clear. A key event for the spatio-temporal regulation of Rho GTPases is their localized activation by the guanine nucleotide exchange factors (GEFs), which promote the exchange of GDP with GTP by Rho GTPases.

GEF-H1, a member of the Dbl family of GEFs, activates Rho GTPases (RhoA, B and C) (Krendel et al., 2002; Ren et al., 1998). Catalytic activity of GEF-H1 is uniquely regulated by its localization to the microtubules (MT). MT depolymerization leads to GEF-H1 activation, while relocalization to MT inhibits its activity (Krendel et al., 2002). Thus, in a number of biological systems, the stimulus-induced disassembly of MT leads to GEF-H1 mediated spatio-temporal activation of RhoA, *e.g.* at the cleavage furrow during cytokinesis, and during cell motility (Birkenfeld et al., 2007; Birkenfeld et al., 2008; Nalbant et al., 2009). Interestingly, in our previous studies, we observed that depletion of GEF-H1 caused aberrant cleavage furrow formation that results in failure of cytokinesis (Birkenfeld et al., 2007) and accumulation of vesicles at the cleavage site indicative of disruption in vesicular traffic. Cells depleted in GEF-H1 also showed defects in both actin dynamics and focal adhesion turnover at the leading edge resulting in a significant defect in cell migration (Nalbant et al., 2009). These defects are dependent on the ability of GEF-H1 to activate Rho GTPase.

In the current study, we have identified the involvement of Rho activating factor GEF-H1 in the regulation of vesicles trafficking pathways of endocytic recycling and exocytosis. We show that GEF-H1 interacts directly with Sec5, a component of exocyst complex, and affects the assembly and/or stability of an exocyst sub-complex and localization of the exocyst components in a GEF-H1 activity-dependent manner. We further report that RalA, a critical regulator of vesicle trafficking, stimulates the interaction between GEF-H1 and Sec5, which in turn is responsible for RhoA activation. Finally, we show that RhoA also plays a direct role in the process of exocytic trafficking by regulating assembly or maintenance of exocyst sub-complex and localization of exocyst protein Exo70 at the PM. Our data define a mechanism for RhoA activation in response to RalA-Sec5 signaling and a function for GEF-H1/RhoA pathway in the regulation of vesicle trafficking.

RESULTS

Perturbation of GEF-H1 function leads to accumulation of vesicular structures

To determine if the role of GEF-H1 in membrane traffic is not just confined to cytokinesis as observed previously (Birkenfeld et al., 2007), we examined the phenotype of control and GEF-H1-depleted cells in non-mitotic phases. Two GEF-H1-targeting siRNA oligonucleotides were used, both of which reduced cellular GEF-H1 levels significantly (Figure S1). The vesicular traffic observed by time lapse microscopy using differential interference contrast (DIC) microscopy showed that loss of GEF-H1 led to accumulation of vesicular structures in the cells (Figures 1A and 1B; 73% and 60% of cells treated with oligos #8 and #9, respectively, Movies S1–3). The phenotype was rescued by expression of siRNA-resistant wild-type protein but not by expression of siRNA-resistant GEF-H1 variant with mutation (Y393A) in the DH domain that abolishes GEF-H1 nucleotide exchange activity (Krendel et al., 2002) (Figures 1C and 1D). To rule out the possibility of phenotype being the result of formation of membrane blebs instead of disruption in vesicular traffic, we

performed thin layer electron microscopy. Accumulation of heterogeneous population of vesicles was observed in 86% of GEF-H1 knockdown cells compared to 17% of control cells (Figure 1E), further confirming the role of GEF-H1 in vesicle trafficking. Therefore, all these results combined suggest a crucial role of GEF-H1 activity in membrane trafficking.

GEF-H1 depletion leads to accumulation of Rab11 positive vesicles

Our results suggest that accumulation of vesicles in GEF-H1-depleted cells could be due to a defect in membrane transport mechanism such as endocytic pathway, including endocytosis and endocytic recycling (Maxfield and McGraw, 2004; Mellman, 1996). To test this hypothesis, we examined the subcellular localization of various proteins that localize to vesicles at different stages of endocytic pathway such as EEA1, an early endosome antigen 1 protein; Rab7, a late endosome protein; LAMP1, a lysosome protein; and Rab11, a recycling endosome and a post-golgi protein marker (Feng et al., 1995; Kornfeld and Mellman, 1989; Stenmark et al., 1996; Ullrich et al., 1996; Urbe et al., 1993). Control and GEF-H1-depleted cells were immunostained for the above mentioned proteins. In control cells, Rab11 localized primarily in a single discreet patch in the perinuclear region that corresponds to the endocytic recycling compartment (ERC) and a few small punctas throughout the cytoplasm (Figure 2A). Interestingly, in GEF-H1-ablated cells, the Rab11 fluorescence associated with small vesicles outside the ERC was enhanced by two-fold (Figures 2A and 2B) compared to control siRNA cells, whereas localization of Rab11 to the ERC was not affected. We did not observe any difference in the localization of EEA1, Rab7 and Lamp1 between control and GEF-H1-knockdown cells (data not shown). These results indicate that a sub-population of vesicles in GEF-H1-depleted cells could be recycling endosomes or post-golgi vesicles.

GEF-H1 depletion affects localization and the recycling of Transferrin

Mis-localization of Rab11 prompted us to study endocytosis and endocytic recycling in GEF-H1-depleted cells to determine whether GEF-H1 plays a role in either receptor internalization and/or recycling. Control and GEF-H1-depleted cells were incubated with fluorescently-labeled transferrin (Tfn) for 10 min to observe ligand internalization. In control cells, the majority of Tfn was found associated with the ERC, with some distributed throughout the cytoplasm (Figure 2C). In GEF-H1-depleted cells, there was 1.5-fold more Tfn scattered throughout the cytoplasm and at the cell periphery compared to control cells (arrow head in Figure 2C). These data suggest that GEF-H1 depletion might increase the uptake and/or diminish the recycling of transferrin receptors (TfR). To test this hypothesis, we first performed kinetic analysis of Tfn uptake (Sever et al., 2000). Cells were incubated with the biotinylated-Tfn, samples were taken out at different time points and the sequestration of Tfn was measured as the amount that remains inaccessible to exogenously added avidin (which masks surface bound biotinylated Tfn). We did not observe any difference in the initial Tfn uptake between the control and GEF-H1-depleted cells (Figure 2D). However, sustained uptake after 10 min led to a gradual decrease in the internalization of the ligand in GEF-H1-depleted cells (Figure 2D). It is possible that during the later time points the uptake is diminished in the absence of GEF-H1 due to a defect in recycling of TfR to the cell surface for uptake of fresh ligand.

We next analyzed the effect of GEF-H1 depletion on recycling of TfR by using fluorescently-labeled Tfn and measuring the kinetics of recycling by fluorescence microscopy. GEF-H1 depletion resulted in the dispersed localization of Tfn after 60 min of steady uptake with incorporation of the ligand in the larger vesicles visible in DIC (e.g. arrow head in Figure 2E). In contrast, in control cells Tfn was predominantly perinuclear (Figure 2E). Furthermore, we observed a slight delay in recycling of receptors to the surface in GEF-H1-depleted cells with a half life of 21.3±1.2 min compared to 17.3±2.3 min for control cells (Figure 2F). These data are statistically significant (p value of 0.05 as

calculated by two-tailed Student's t-test). Our results indicate a defect in localization of Tfn and a slight delay in recycling through the ERC in absence of GEF-H1.

GEF-H1 regulates exocytic pathway

To gain further information into the involvement of GEF-H1 in membrane trafficking pathways, we next investigated its role in the process of exocytosis by using the secretory reporter vesicular stomatitis virus temperature-sensitive variant ts045 (GFP-VSV-G^{ts045}). At restrictive temperature VSV-G^{ts045} is retained within the ER, then upon shift to permissive temperature moves as a synchronous population through the golgi to the PM (Hirschberg et al., 1998). We used GFP-VSV-G to visualize its transport within the cells, while incorporation into the PM was detected by immunostaining with 8G5 mAb against the extracellular domain of the protein, without permeabilization (Lefrancois and Lyles, 1982). GFP fluorescence revealed that most of VSV-G protein was localized in the golgi complex within 30 min of shift to permissive temperature in both control and GEF-H1-depleted cells indicating that trafficking from ER to golgi was not affected by GEF-H1 depletion (Figure 3A). Interestingly, we observed a two-fold less insertion of VSV-G at the PM in GEF-H1-depleted cells compared to control cells indicating a delay in the transport from golgi to the PM (time points 60–90 min) (Figures 3A and 3B). These results suggest a positive role for GEF-H1 in regulation of exocytosis.

To further investigate this possibility, we examined the effect of GEF-H1 (wt, microtubule binding-deficient variant (C53R) that is constitutively active (Krendel et al., 2002), and inactive Y393A variant) overexpression on GFP-VSV-G ^{ts045} trafficking. We observed that in all conditions VSV-G transport from ER to golgi was not affected (Figure 3C, time point 30 min). However, cells overexpressing GEF-$H1^{wt}$ showed an increase of VSV-G at the PM (Figures 3C and 3D; 35% more fluorescence intensity of 8G5 at the PM after 60 min compared to empty vector control cells). Expression of GEF-$H1^{C53R}$ led to a further increase in the appearance of VSV-G on the surface (up to 55% more fluorescence intensity compared to empty vector control cells) (Figures 3C and 3D). In contrast, overexpression GEF-$H1^{Y393A}$ mutant caused a decrease in the insertion of VSV-G protein at the PM by 20% as compared to control cells (Figures 3C and 3D). Therefore, we conclude that GEF-H1 exerts a positive influence on VSV-G trafficking from golgi to PM through its catalytic activity. Together, these results demonstrate that GEF-H1 is involved in both endocytic recycling and exocytosis.

GEF-H1 depletion perturbs the localization of exocyst components Exo70 and Sec8 and affects the complex assembly/stability

Since the defect in GEF-H1 activity leads to disruption of both endocytic recycling and exocytosis, we hypothesized that GEF-H1 might control the later stages of membrane trafficking. The exocyst complex plays a crucial role in tethering and fusion of vesicles at the PM and disruption of its function leads to defects in secretion and accumulation of vesicles (He and Guo, 2009; Wu et al., 2008). Therefore, we decided to investigate the possibility that disruption in vesicle trafficking in the absence of GEF-H1 could be associated with exocyst function. To test this hypothesis, we examined the localization of exocyst components in GEF-H1-depleted cells. Due to the availability of antibodies, we determined the localization of exocyst protein Exo70 in control and GEF-H1-depleted cells. In control cells, Exo70 localized both at the PM and on vesicular structures in the cytoplasm (Figure 4A) similar to what was observed in yeast (Boyd et al., 2004). Interestingly, we observed an increase in the accumulation of Exo70-positive vesicles at the periphery of GEF-H1-ablated cells (Figure 4A). Quantification of the number of vesicles/cell revealed that 50% of GEF-H1-depleted cells have more than 40 vesicles/cell compared to only 10% of control cells (Figure 4B). Since Exo70 has been suggested to serve as the docking point

for assembly of the complete exocyst complex at the membrane (Liu et al., 2007), we examined the localization of other components of exocyst complex such as Sec8. We observed that in control cells, more than 70% of cells exhibited Sec8 localization to both the cell leading edge and cytoplasm, whereas in GEF-H1-depleted cells, only 30% of cells showed Sec8 localization to the cell edge (Figures 4C and 4D). The loss of Sec8 PM localization was not due to the differences in membrane morphology between control and GEF-H1-depleted cells as distribution of membrane protein Na^+K^+ATPase was not altered by GEF-H1 ablation (Figure S2). We also observed a more dispersed localization of Sec8 in GEF-H1-depleted cells as compared to control cells (Figure 4C). These data indicate that the loss of GEF-H1 perturbs Exo70 and subsequently Sec8 localization.

Studies done in yeast suggest that the formation of a complex between components present on vesicles with the rest of exocyst constituents at the PM is critical for directing vesicle traffic (Guo et al., 2000). Therefore, we examined the effect of GEF-H1 expression constructs (GEF-$H1^{wt}$, Y393A (constitutively inactive) or C53R (constitutively active)) on assembly of such a sub-complex between Sec8 and Exo70 in immunoprecipitation experiments. Immunoblot analysis of the precipitation of endogenous Sec8 revealed that overexpression of GEF-$H1^{wt}$ led to a significant increase in association between Sec8 and Exo70 proteins compared to cells expressing empty vector; this effect was further enhanced by expression of GEF-$H1^{C53R}$ variant (Figures 4E and 4F). Interestingly, the association between Sec8 and Exo70 was reduced by approximately 40% in cells expressing inactive GEF-$H1^{Y393A}$ variant when compared to cells with empty vector (Figures 4E and F). Thus, together, these results strongly support a role of GEF-H1 activity in regulating the localization of exocyst proteins to the PM and the complex assembly and/or stability.

GEF-H1 interacts directly with exocyst protein Sec5

We identified an interaction between GEF-H1 and exocyst using mass spectrometry analysis. We confirmed the interaction between GEF-H1 and Sec5 by pull-down experiments in HeLa cells co-expressing EGFP-GEF-H1 and HA-Sec5 (Figure 5A). To determine the region of GEF-H1 that binds to Sec5, we used a panel of recombinant purified truncated GST-GEF-H1 mutants, (described in Figure 5B, bottom panel) and performed GST pull-down assays with lysates from HeLa cells expressing HA-Sec5. We found that the C-terminal constructs (462–570 and 572–985 constructs 3 and 4, Figure 5B lane 4 and 5, respectively) failed to interact with HA-Sec5 while the N-terminal constructs (1–236 and 237–467 constructs 1 and 2, respectively) demonstrated interaction with HA-Sec5 (Figure 5B, lane 2 and 3, respectively). We further mapped the region of GEF-H1 interacting with Sec5 by using shorter N-terminal regions of GEF-H1 (Figure 5B, constructs 5–9, lanes 6–10). Constructs 10 and 11 (amino acids 200–236 and 220–250, respectively) did not interact with HA-Sec5 (Figure 5B, lanes 11 and 12), while construct 9 (amino acids 119–236) co-precipitated efficiently with HA-Sec5 (Figure 5B, lane10). These data indicate that the critical GEF-H1-binding region is within amino acid residues 119–200. We next determined whether GEF-H1 could directly interact with Sec5. Since Sec5 is a high molecular weight protein it is difficult to express in *E.coli*, thus, we produced HA-Sec5 protein using the Promega TNT-T7 *in vitro* reticulocyte lysate expression system. We then incubated the *in vitro* translated HA-Sec5 protein with purified GST or GST tagged fragments of GEF-H1 (described in Figure 5C bottom panel) and assayed for co-precipitation between Sec5 and GST proteins by GST-pulldown. As shown in Figure 5C, only GEF-H1(aa119–236) bound directly to Sec5 while no co-precipitation was observed with GST alone or other regions of GEF-H1.

We next examined whether the binding of GEF-H1 to Sec5 is dependent on the ability of GEF-H1 to interact with MT. HeLa cells were co-transfected with HA-Sec5 and either GFP empty vector, GFP-GEF-$H1^{wt\ or\ C53R}$. HA-Sec5 was immunoprecipitated using HA

antibody and assayed for GFP-GEF-H1 interaction. As shown in Figure 5D, the MT binding-deficient GEF-H1 mutant showed high *in vivo* binding to Sec5 compared to GFP-GEF-H1^{wt} while no interaction was observed with GFP empty vector.

Since depletion of GEF-H1 affects Exo70 localization, we examined if GEF-H1 and Exo70 might be part of a complex. We expressed HA-Exo70 in HeLa cells and assayed the lysates for co-precipitation with recombinant purified truncated versions of GST-GEF-H1 protein by GST pull-down as described above. We observed an interaction of Exo70 with the N-terminal region of GEF-H1 (amino acids between 1–236, Figure S3A, lane 2), the DH and the phospholipid-binding domains (Figure S3A, lanes 3 and 4, respectively) while the C-terminal regions (Figure S3A, lane 5) and GST protein alone did not precipitate Exo70. However, we did not detect a direct interaction between *in vitro* translated Exo70 and purified recombinant GST-GEF-H1 (Figure S3B). Since the critical region of GEF-H1 required to pull-down Exo70 in HeLa cells was the same region that bound directly to Sec5 it is likely that Exo70 interacts with GEF-H1 via Sec5 or other exocyst components.

Next, we determined if the binding between exocyst and GEF-H1 contributes to its role in vesicle trafficking. To accomplish this we disrupted the interaction between endogenous GEF-H1 and Sec5 by overexpression of competing GST-GEF-H1$^{(aa119–236)}$ peptide and examined the effect on secretion of GFP-VSV-G. As expected, the cells expressing GST-tagged competing peptide exhibited an accumulation of GFP-VSV-G vesicles and more than 40% decrease in the insertion of VSV-G at the PM compared to the GST empty vector (Figures 5E and 5F). Moreover, we observed that actin cytoskeleton of cells expressing GST-GEF-H1$^{(aa119–236)}$ peptide or GST empty vector was not perturbed (Figure S3C). Thus we conclude that the direct interaction between GEF-H1 and exocyst protein Sec5 is crucial for the role of GEF-H1 in membrane trafficking.

Ral GTPases affect the interaction between GEF-H1 and Sec5 and the activation of Rho GTPase

We next determined the molecular mechanism controlling the interaction between Sec5 and GEF-H1. Ral GTPases have been shown to regulate the assembly of exocyst complex by direct interaction with two distinct subunits, Sec5 and Exo84 (Jin et al., 2005; Moskalenko et al., 2002). Since GEF-H1 interacts with Sec5 *in vivo,* we next examined the effect of RalA expression on the interaction between endogenous GEF-H1 and Sec5 by immunoprecipitation. As shown in Figure 6A and 6B, overexpression of RalA^{wt} enhanced the interaction between GEF-H1 and Sec5 by 2-fold compared to the empty vector control. The effect of constitutively active variant RalA$^{(G23V)}$ and the fast-cycling active mutant RalA$^{(F39L)}$ was even more dramatic than Ral^{wt} (Figure 6A and 6B; 5 and 6-fold increase in GEF-H1-Sec5 interaction compared to control, respectively). This data is consistent with the fact that the fast-cycling mutant blocks Sec5 dimerization facilitating its interaction with other effectors (Chien et al., 2006). Next, to assess the biological role of RalA-Sec5-GEF-H1 interaction, we characterized the consequences on GEF-H1 activity by examining the effect of RalA constructs on the activation of RhoA using a Rhotekin RBD (Rho-binding domain) pull-down assay (Stofega et al., 2006). HeLa cells expressing either empty vector or various constructs of RalA as mentioned in Figure 6C were treated with DMSO. HeLa cells treated with Nocodazole were used as positive control for RhoA activation. We observed a 3-fold increase in the levels of active RhoA (normalized to total RhoA expression level) in cells expressing RalA^{wt} or RalA^{G23V} compared to control cells. These levels were four-fold higher when cells expressed RalA^{F39L} (Figures 6C and 6D). Intriguingly, RalA mutant (RalA^{E38R}) that cannot interact with Sec5 was not able to mediate activation of RhoA, whereas RalA^{A48W} that can bind to Sec5, but not Exo84 (Jin et al., 2005), facilitated RhoA activation compared to cells with empty vector (Figures 6C and 6D). This effect of RalA on RhoA activation was abolished in GEF-H1 depleted cells

(Figures 6E and 6F). These data strongly suggest that RalA promotes the interaction of Sec5 with GEF-H1 and regulates RhoA activation. To confirm this, we tested the effect of RalA on RhoA activation in cells expressing the peptide fragment of GEF-H1 (aa119–236) involved in binding with Sec5. Weco -expressed GEF-H1$^{(119–236)}$ or empty vector with either Ral^{G23V} or Ral^{F39L} in HeLa cells, then using RBD pull-down assays, we found that cells expressing either Ral^{G23V} or Ral^{F39L} with empty vector increased RhoA activation by four-fold and two-fold, respectively, compared to cells expressing empty vector alone. Interestingly, cells expressing Ral^{G23V} or Ral^{F39L} in presence of GEF-H1$^{(119–236)}$ showed no enhancement in RhoA activation (Figures 6G and 6H). These results indicate that RalA mediates RhoA activation *via* the interaction between GEF-H1 and Sec5. Altogether, these results strongly implicate Ral GTPase in the regulation of the interaction between Sec5 and GEF-H1 and subsequently in RhoA activation.

Rho GTPase regulates exocyst assembly and localization

Our results prompted us to investigate the role of RhoA in exocyst function. We first determined whether RhoA interacts with the exocyst complex. We co-expressed in HeLa cells, HA-Sec5 with either GFP-RhoA^{wt}, RhoA^{Q63L} or RhoA^{T19N}. Immunoblot analyses of Sec5 precipitation and quantification of the data revealed that RhoA^{wt} exhibited a 10-fold higher interaction with Sec5 as compared to RhoA^{Q63L} and RhoA^{T19N}, suggesting that the catalytic cycling of RhoA is important for the interaction (Figure 7A and 7B). Next, we determined whether Rho function is important for exocyst complex assembly or maintenance by examining the effect of RhoA^{wt} and variants on the interaction between Exo70 and Sec8. Immunoblot analysis revealed a significant increase in the association between Sec8 and Exo70 in the presence of RhoA^{wt}, but not with RhoA^{Q63L} or RhoA^{T19N} (Figures 7C and 7D). This result indicates that RhoA catalytic cycle plays a positive role in directing exocyst assembly/maintenance.

Next, we wanted to examine if similar to GEF-H1, RhoA and/or RhoB influence the localization of exocyst component Exo70. We depleted RhoA alone or in combination with RhoB, since RhoB has been shown to compensate for the loss of RhoA (Ho et al., 2008) (Figure S5C), and examined the effect on localization of Exo70 by immunofluorescence. As shown in Figure 7E, we observed a significant increase in the number of cells with accumulation of Exo70-positive vesicles at the periphery in RhoA-depleted cells compared to control cells. Quantification shown in Figure 7F revealed that around 50% of RhoA-depleted cells had more than 40 vesicles/cell compared to 11% of control cells. Simultaneous ablation of both RhoA and B showed only a slight increase in the accumulation of vesicles compared to RhoA depletion alone (approximately 60% of double-depleted cells exhibited >40 vesicles/cell) (Figures 7E and 7F). This data strongly involves RhoA, in the regulation of the assembly/stability and localization of the exocyst complex.

As a result of Rho's involvement in exocyst localization and assembly, we next investigated the effect of Rho GTPases on vesicle trafficking by determining the effect of inhibition of Rho activity on VSV-G transport. As observed by GFP fluorescence inhibition of RhoA, B and C isoforms by C3 transferase did not affect the trafficking of VSV-G from ER to golgi (Figure 7G, time point 30min). However, there was a significant decrease in the insertion of VSV-G at the PM (40% decrease in the intensity of 8G5 staining compared to control cells) (Figure 7G). Furthermore, we also examined the effect of dominant negative RhoA$^{(T19N)}$ or RhoB$^{(T19N)}$ on the incorporation of VSV-G at the PM (Figures S4A and S4C). VSV-G insertion into the PM revealed by immunostaining with 8G5 antibody was significantly reduced by approximately 40% in cells expressing RhoA$^{(T19N)}$ (Figures S4A and S4B) and by 30% in cells expressing RhoB$^{(T19N)}$ cells (Figures S4C and S4D) compared to cells with empty vector (time points 60–90 min). These results further emphasize the requirement of Rho activity for vesicle targeting. Moreover, since dominant negative Rho GTPase mutants

sequester the GEFs and preclude their accessibility to other Rho GTPases, these results may also emphasize the role of GEF-H1 in the process of vesicle trafficking.

To identify which isoforms of Rho are required for the vesicle trafficking, we next depleted RhoA, RhoB and RhoC individually or in combination (Figure S5C and S5F) and examined the effect on VSV-G trafficking to the PM. Incorporation of VSV-G at the PM was negatively affected by RhoA depletion (approximately 25% reduction in intensity of 8G5 staining compared to control siRNA cells at 80 and 90 min) and to a larger extent by RhoA and B co-depletion (40% decrease in the intensity of 8G5 staining compared to control siRNA cells at 80 and 90 min) (Figures 7H and 7I). Interestingly, depletion of RhoB alone did not show any effect on VSV-G trafficking to the PM (Figure S5A and S5B). Since, in RhoA-depleted cells RhoB protein levels increase considerably (Figure S5C) it can possibly substitute for RhoA's function as has been described previously, explaining the enhanced effect of RhoA and B co-depletion on VSV-G trafficking compared to cells depleted in RhoA alone. Depletion of RhoC individually did not show any effect on VSV-G trafficking to the PM (Figure S5A and S5B). Localization of VSV-G at the PM in cells simultaneously depleted in RhoA, B and C was similar to that of RhoA and B co-depletion (approximately 40% less staining with 8G5 antibody at 60 and 90 min compared to control cells) (Figures S5D and S5E) indicating that RhoC is not involved in the VSV-G trafficking. Thus we conclude that RhoA is the primary Rho GTPase involved in vesicle trafficking to the PM, while RhoB can substitute partially in absence of RhoA when RhoB levels are elevated.

DISCUSSION

We have identified a mechanism for RhoA activation and a function of GEF-H1/RhoA signaling pathway in membrane trafficking which has important implications for its role in cell division and migration (Caswell and Norman, 2008; Prekeris and Gould, 2008; Wittmann and Waterman-Storer, 2001). Depletion of GEF-H1 leads to accumulation of heterogeneous population of vesicles in cells as observed by DIC as well as thin layer electron microscopy suggesting that the structures observed under DIC are in fact vesicles and not membrane blebs. Furthermore, some of the vesicles co-localized with labeled Tfn and we observed defect in both endocytic recycling and exocytosis (we also observed accumulation of GFP-VSV-G vesicles) suggesting a role for GEF-H1 in the common terminal steps of vesicle tethering and fusion at the PM. Significant evidence implicate the exocyst complex as a critical player in targeted delivery and tethering/fusion of vesicles at the PM.

Our results show that GEF-H1 interacts with exocyst components, and is critical for specific localization of Exo70 and Sec8. GEF-H1 is also involved in the formation of a complex between the two proteins which in turn will have direct impact on the exocyst complex localization. Depletion of GEF-H1 leads to accumulation of Exo70-positive vesicles, frequently near the PM, suggesting a defect in tethering of these vesicles at the surface. The catalytic activity of GEF-H1 is crucial for its role in membrane trafficking as the dominant negative variant of GEF-H1^{Y393A} exhibited vesicle accumulation similar to GEF-H1-depleted cells. GEF-H1^{Y393A} expression also leads to a significant reduction in the association between Sec8 and Exo70, which is reflected in delay observed in VSV-G exocytosis. Conversely, constitutively active GEF-H1^{C53R} stimulated the interaction between the exocyst components and enhanced exocytosis of VSV-G. GEF-H1^{C53R} also shows stronger interaction with Sec5 than GEF-H1^{wt} suggesting that Sec5 binds more efficiently to free GEF-H1, and might even facilitate extraction of GEF-H1 from the MT.

Our results provide strong evidence that RalA stimulates the interaction between GEF-H1 and Sec5. Furthermore, RalA expression regulates RhoA activation in Sec5/GEF-H1-

dependent manner. RalA has been shown to regulate the activity of Rho family members Rac and Cdc42, but not RhoA through its effector RLIP76, which acts as a GTPase-activating protein (Jullien-Flores et al., 1995). Rho GTPase protein level increases concurrent with Ral activation in response to EGF stimulation of human tumor cell lines harboring activated HA-RasV12 (Gildea et al., 2002). Now, we have shown that RalA directly modulates of RhoA activity through its effector Sec5.

Rho GTPases play a crucial role in regulating actin dynamics and membrane trafficking (Ridley, 2001). However, their roles in regulating vesicle trafficking and fusion at the PM are not well understood. Evidence from Rho family GTPase TC10 that regulates exocytosis of GLUT4-containing vesicles suggests that interaction with exocyst and GTP hydrolysis are important for exocytic vesicle fusion (Kanzaki and Pessin, 2003; Kawase et al., 2006). In Yeast, Rho GTPases regulate the polarized localization of exocyst component Sec3, and activation of the exocyst complex at the PM to facilitate vesicle fusion (Guo et al., 2001; Wu et al., 2008). Similarly, in mammalian systems also RhoA may regulate exocyst function for targeting vesicles to the sites of secretion. Our studies provide evidence that RhoA activity controls exocyst function by positively affecting the association between Exo70 and Sec8 and the localization of Exo70. Therefore, RhoA regulates the golgi-PM trafficking in a way similar to what we observed with GEF-H1. It is interesting to observe that the direct interaction between GEF-H1 and Sec5 is crucial for RhoA activation in response to Ral as well as for vesicle trafficking without causing observable changes in the actin cytoskeleton (Figure S3C). Thus it is likely that GEF-H1 affects membrane trafficking primarily via interaction with exocyst, although involvement of GEF-H1/Rho pathway in modulation of actin cytoskeleton might also play some role in the process of vesicle targeting. Thus, it raises an interesting possibility that the GEF-H1-Rho signaling pathway can coordinate cytoskeletal modulation with membrane trafficking and vesicle fusion.

Thus, based on our results, we suggest a model in which a RalA-exocyst complex facilitates the activation of RhoA by GEF-H1, for example by localizing delivery of GEF-H1 to specific sites. RhoA in turn regulates exocyst function by affecting its localized recruitment and/or activation at the PM to facilitate the complex formation.. Our data provide evidence of a mechanism for activation of RhoA by Ral-exocyst-GEF-H1 signaling event which in turn affects vesicle trafficking via regulation of exocyst function. We propose GEF-H1 as a key protein that can regulate the coordination between MT and actin cytoskeleton, and vesicle trafficking.

EXPERIMENTAL PROCEDURES

Electron microscopy

HeLa cells plated on plastic bottom dishes were transfected with 20nM control siRNA or GEF-H1 siRNA using Lipofectamine RNAi Max (Invitrogen). 72 hrs post-transfection, cells were processed using the Gilula *et al.* method (Gilula et al., 1978) (see Supplemental Methods for detailed).

Tfn internalization and recycling assays

HeLa cells transfected with control or GEF-H1 specific siRNA were plated on FN coated glass coverslips after 48 hrs. Next day, the cells were serum starved for 2 hrs before incubating them in medium containing 15 μg/ml alexa fluor 568 conjugated Tfn (Molecular probes, Eugene, OR) for 10 min at 37°C. The cells were then washed with PBS and incubated in acid stripping buffer (0.2M Acetic acid, 0.5M NaCl, pH 2.8) for 2 min on ice to remove surface bound ligand. Samples were then neutralized by washing with PBS and fixed with 4% PFA, mounted on glass slides and observed under fluorescence microscope.

The kinetics of Tfn uptake was measured after 72 hrs of GEF-H1 depletion by using biotinylated Tfn as described earlier (Sever et al., 2000). Briefly, cells were detached using 5 mM EDTA in PBS buffer and incubating at 37°C for 5 min. Cells were then washed briefly with PBS and resuspended in ice-cold buffer containing 1 mM $MgCl_2$, 1 mM $CaCl_2$, 0.2% BSA, 5mM glucose and 5 μg/ml biotinylated-Tfn (Molecular probes, Eugene, OR) at density of 2×10^6 cells/ml. Cells were then split into 50 μl aliquots on ice and internalization of Tfn was triggered by incubating the samples in 37°C water bath for appropriate time intervals. The samples for time point 0 min and "total Tfn" (indicating the total amount of labeled-Tfn bound to the cells) were kept on ice for the duration of the experiment. Internalization of Tfn was stopped by transferring the samples to ice, which stops endocytosis. The samples, including time point 0min were washed once with cold PBS and resuspended in 100 μl of PBS containing 0.2% BSA and 50 μg/ml avidin (Sigma) and then incubated on a tube shaker for 1 hr at 4°C to mask the surface-bound Tfn. The reaction was then quenched by the addition of 10 μl of 0.5 mg/ml biocytin (sigma) and incubated again for 10 min at 4°C on tube shaker. All the samples including "total Tfn" were solubilized by addition of blocking buffer (2.9 mg/ml NaCl, 1.6 mg/ml Tris-HCl pH 7.6, 3.7 mg/ml EDTA, final pH 7.4) and vortexing. After incubating on ice for 5–10 min the samples were transferred to ELISA plates coated with α-Tfn antibody (whole serum produced in goat, Sigma). The plates were incubated overnight at 4°C. The wells were then washed three times with PBS and developed using 200 μl assay buffer (10mg *o*-phenylenediamine, 10 μl of 30% H_2O_2 in 25 ml of citrate buffer containing 50 mM Na_2HPO_4, 27 mM citrate, pH 5) and incubating at room temperature to develop color, for approximately 2–4 min. This reaction was terminated by the addition of 50 μl 2M H_2SO_4 per well. The absorbance was measured at 490 nm and corrected for 650 nm. The amount of Tfn internalized at different time points was expressed as percentage of total Tfn bound to the cells.

We used fluorescently-labeled Tfn and measured the kinetics of recycling by fluorescence microscopy, instead of biotinylated-Tfn due to difficulties associated with incubating the cells at 4°C for prolonged periods of time for masking the surface bound biotinylated-Tfn with avidin. GEF-H1-depleted and control cells were plated on glass coverslips and serum starved for 2 hrs. Samples were then incubated with 15 μg/ml of fluorescently labeled Tfn for 1 hr at 37°C. The samples were then washed with PBS and fresh medium containing 15 μg/ml unlabeled Tfn (Sigma) was added to drive the Tfn recycling process, and incubated at 37°C. Samples were taken out at indicated time points, acid washed to remove surface bound ligand, fixed with PFA and observed using fluorescence microscope. Amount of Tfn retained within the cells at various time points was quantified and expressed as the percentage of total internalized Tfn at t=0. The rate of decay was determined by fitting the natural log of the ratio of average fluorescence intensity of Tfn retained within the cells at time t over the average fluorescence intensity at the start of the experiment to a linear dependence on time. The slope is the rate of decay. The half life was calculated as the natural log of 2 divided by the rate of decay.

Exocytosis assays

siRNA transfected cells were plated on FN coated glass coverslips after 48 hrs. Cells were then transfected with GFP-VSV-G^{ts045} and incubated further for 20 hrs at 40°C. For analysis of the effect of GEF-H1 overexpression on exocytosis, WT and variants of GEF-H1 were co-transfected with GFP-VSV-G^{ts045} for 20 hrs. All subsequent incubations at the permissive temperature (32°C) were done in the presence of 50 μg/ml cycloheximide (Sigma) to halt protein synthesis. After taking a sample at t=0 the cells were shifted to 32°C and samples were taken at indicated time points and fixed with 4% PFA. Cells were stained with mouse monoclonal anti-VSV-G (8G5) antibody without permeabilization to visualize

the insertion of VSV-G in the PM. Trafficking of VSV-G through ER to the PM was visualized using GFP fluorescence. The samples were observed using confocal microscope.

In vitro translation and binding assay

To determine whether the binding between GEF-H1 and Sec5 or Exo70 was direct, recombinant GST-GEF-H1 fragments spanning the entire sequence of GEF-H1 were used. HA-rSec5 and HA-rExo70 were *in vitro* translated (Promega TNT Quick Coupled) for 90 min at 30°C. 12 μl was used in each binding reaction. Extracts were incubated in binding buffer containing 50 mM Tris pH 7.4, 150 mM NaCl, and 1.0% NP-40 for 2 hrs at 4° C. Samples were washed 3x in binding buffer and resolved by SDS-PAGE gel and immunoblotted with anti-HA antibody.

Pull-down assay

Cells transfected with appropriate plasmids were lysed and RBD pull-down assay was performed as described earlier (Stofega et al., 2006). For nocodazole (Sigma-Aldrich, St. Louis, Mo) treatment, cells were incubated with either DMSO or 10 μM nocodazole for 45 min at 37°C.

Supplementary Material

Refer to Web version on PubMed Central for supplementary material.

Acknowledgments

We dedicate this manuscript to the memory of late Dr. Gary Bokoch without whose support and guidance this work would not have been possible. We thank Charles Yeaman, Rytis Prekeris, Jennifer Lippincott-Schwartz, Klaus Hahn and Douglas Lyles for some of the reagents used in this study. We also thank Charles Yeaman for helpful suggestions and advice and Brufce Fowler for assistance with preparation of some DNA constructs. This study was supported by NIH grant to GMB and CDM (GM39434).

References

Birkenfeld J, Nalbant P, Bohl BP, Pertz O, Hahn KM, Bokoch GM. GEF-H1 modulates localized RhoA activation during cytokinesis under the control of mitotic kinases. Dev Cell. 2007; 12:699–712. [PubMed: 17488622]

Birkenfeld J, Nalbant P, Yoon SH, Bokoch GM. Cellular functions of GEF-H1, a microtubule-regulated Rho-GEF: is altered GEF-H1 activity a crucial determinant of disease pathogenesis? Trends Cell Biol. 2008; 18:210–219. [PubMed: 18394899]

Boyd C, Hughes T, Pypaert M, Novick P. Vesicles carry most exocyst subunits to exocytic sites marked by the remaining two subunits, Sec3p and Exo70p. J Cell Biol. 2004; 167:889–901. [PubMed: 15583031]

Caswell P, Norman J. Endocytic transport of integrins during cell migration and invasion. Trends Cell Biol. 2008; 18:257–263. [PubMed: 18456497]

Chang YC, Nalbant P, Birkenfeld J, Chang ZF, Bokoch GM. GEF-H1 couples nocodazole-induced microtubule disassembly to cell contractility via RhoA. Mol Biol Cell. 2008; 19:2147–2153. [PubMed: 18287519]

Chien Y, Kim S, Bumeister R, Loo YM, Kwon SW, Johnson CL, Balakireva MG, Romeo Y, Kopelovich L, Gale M Jr, et al. RalB GTPase-mediated activation of the IkappaB family kinase TBK1 couples innate immune signaling to tumor cell survival. Cell. 2006; 127:157–170. [PubMed: 17018283]

Feng Y, Press B, Wandinger-Ness A. Rab 7: an important regulator of late endocytic membrane traffic. J Cell Biol. 1995; 131:1435–1452. [PubMed: 8522602]

Fielding AB, Schonteich E, Matheson J, Wilson G, Yu X, Hickson GR, Srivastava S, Baldwin SA, Prekeris R, Gould GW. Rab11-FIP3 and FIP4 interact with Arf6 and the exocyst to control membrane traffic in cytokinesis. EMBO J. 2005; 24:3389–3399. [PubMed: 16148947]

Gildea JJ, Harding MA, Seraj MJ, Gulding KM, Theodorescu D. The role of Ral A in epidermal growth factor receptor-regulated cell motility. Cancer Res. 2002; 62:982–985. [PubMed: 11861368]

Gilula NB, Epstein ML, Beers WH. Cell-to-cell communication and ovulation. A study of the cumulus-oocyte complex. J Cell Biol. 1978; 78:58–75. [PubMed: 670298]

Gromley A, Yeaman C, Rosa J, Redick S, Chen CT, Mirabelle S, Guha M, Sillibourne J, Doxsey SJ. Centriolin anchoring of exocyst and SNARE complexes at the midbody is required for secretory-vesicle-mediated abscission. Cell. 2005; 123:75–87. [PubMed: 16213214]

Guo W, Sacher M, Barrowman J, Ferro-Novick S, Novick P. Protein complexes in transport vesicle targeting. Trends Cell Biol. 2000; 10:251–255. [PubMed: 10802541]

Guo W, Tamanoi F, Novick P. Spatial regulation of the exocyst complex by Rho1 GTPase. Nat Cell Biol. 2001; 3:353–360. [PubMed: 11283608]

He B, Guo W. The exocyst complex in polarized exocytosis. Curr Opin Cell Biol. 2009; 21:537–542. [PubMed: 19473826]

Hirschberg K, Miller CM, Ellenberg J, Presley JF, Siggia ED, Phair RD, Lippincott-Schwartz J. Kinetic analysis of secretory protein traffic and characterization of golgi to plasma membrane transport intermediates in living cells. J Cell Biol. 1998; 143:1485–1503. [PubMed: 9852146]

Ho TT, Merajver SD, Lapiere CM, Nusgens BV, Deroanne CF. RhoA-GDP regulates RhoB protein stability. Potential involvement of RhoGDIalpha. J Biol Chem. 2008; 283:21588–21598. [PubMed: 18524772]

Jin R, Junutula JR, Matern HT, Ervin KE, Scheller RH, Brunger AT. Exo84 and Sec5 are competitive regulatory Sec6/8 effectors to the RalA GTPase. EMBO J. 2005; 24:2064–2074. [PubMed: 15920473]

Jullien-Flores V, Dorseuil O, Romero F, Letourneur F, Saragosti S, Berger R, Tavitian A, Gacon G, Camonis JH. Bridging Ral GTPase to Rho pathways. RLIP76, a Ral effector with CDC42/Rac GTPase-activating protein activity. J Biol Chem. 1995; 270:22473–22477. [PubMed: 7673236]

Kanzaki M, Pessin JE. Insulin signaling: GLUT4 vesicles exit via the exocyst. Curr Biol. 2003; 13:R574–576. [PubMed: 12867054]

Kawase K, Nakamura T, Takaya A, Aoki K, Namikawa K, Kiyama H, Inagaki S, Takemoto H, Saltiel AR, Matsuda M. GTP hydrolysis by the Rho family GTPase TC10 promotes exocytic vesicle fusion. Dev Cell. 2006; 11:411–421. [PubMed: 16950130]

Kornfeld S, Mellman I. The biogenesis of lysosomes. Annu Rev Cell Biol. 1989; 5:483–525. [PubMed: 2557062]

Krendel M, Zenke FT, Bokoch GM. Nucleotide exchange factor GEF-H1 mediates cross-talk between microtubules and the actin cytoskeleton. Nat Cell Biol. 2002; 4:294–301. [PubMed: 11912491]

Lefrancois L, Lyles DS. The interaction of antibody with the major surface glycoprotein of vesicular stomatitis virus. II. Monoclonal antibodies of nonneutralizing and cross-reactive epitopes of Indiana and New Jersey serotypes. Virology. 1982; 121:168–174. [PubMed: 6180551]

Liu J, Zuo X, Yue P, Guo W. Phosphatidylinositol 4,5-bisphosphate mediates the targeting of the exocyst to the plasma membrane for exocytosis in mammalian cells. Mol Biol Cell. 2007; 18:4483–4492. [PubMed: 17761530]

Maxfield FR, McGraw TE. Endocytic recycling. Nat Rev Mol Cell Biol. 2004; 5:121–132. [PubMed: 15040445]

Mellman I. Endocytosis and molecular sorting. Annu Rev Cell Dev Biol. 1996; 12:575–625. [PubMed: 8970738]

Montagnac G, Echard A, Chavrier P. Endocytic traffic in animal cell cytokinesis. Curr Opin Cell Biol. 2008; 20:454–461. [PubMed: 18472411]

Moskalenko S, Henry DO, Rosse C, Mirey G, Camonis JH, White MA. The exocyst is a Ral effector complex. Nat Cell Biol. 2002; 4:66–72. [PubMed: 11740492]

Nalbant P, Chang YC, Birkenfeld J, Chang ZF, Bokoch GM. Guanine nucleotide exchange factor-H1 regulates cell migration via localized activation of RhoA at the leading edge. Mol Biol Cell. 2009; 20:4070–4082. [PubMed: 19625450]

Novick P, Guo W. Ras family therapy: Rab, Rho and Ral talk to the exocyst. Trends Cell Biol. 2002; 12:247–249. [PubMed: 12074877]

Oztan A, Silvis M, Weisz OA, Bradbury NA, Hsu SC, Goldenring JR, Yeaman C, Apodaca G. Exocyst requirement for endocytic traffic directed toward the apical and basolateral poles of polarized MDCK cells. Mol Biol Cell. 2007; 18:3978–3992. [PubMed: 17686995]

Prekeris R, Gould GW. Breaking up is hard to do - membrane traffic in cytokinesis. J Cell Sci. 2008; 121:1569–1576. [PubMed: 18469013]

Prigent M, Dubois T, Raposo G, Derrien V, Tenza D, Rosse C, Camonis J, Chavrier P. ARF6 controls post-endocytic recycling through its downstream exocyst complex effector. J Cell Biol. 2003; 163:1111–1121. [PubMed: 14662749]

Ren Y, Li R, Zheng Y, Busch H. Cloning and characterization of GEF-H1, a microtubule-associated guanine nucleotide exchange factor for Rac and Rho GTPases. J Biol Chem. 1998; 273:34954–34960. [PubMed: 9857026]

Ridley AJ. Rho proteins: linking signaling with membrane trafficking. Traffic. 2001; 2:303–310. [PubMed: 11350626]

Sever S, Damke H, Schmid SL. Dynamin:GTP controls the formation of constricted coated pits, the rate limiting step in clathrin-mediated endocytosis. J Cell Biol. 2000; 150:1137–1148. [PubMed: 10974001]

Stenmark H, Aasland R, Toh BH, D'Arrigo A. Endosomal localization of the autoantigen EEA1 is mediated by a zinc-binding FYVE finger. J Biol Chem. 1996; 271:24048–24054. [PubMed: 8798641]

Stofega M, DerMardirossian C, Bokoch GM. Affinity-based assay of Rho guanosine triphosphatase activation. Methods Mol Biol. 2006; 332:269–279. [PubMed: 16878699]

Ullrich O, Reinsch S, Urbe S, Zerial M, Parton RG. Rab11 regulates recycling through the pericentriolar recycling endosome. J Cell Biol. 1996; 135:913–924. [PubMed: 8922376]

Urbe S, Huber LA, Zerial M, Tooze SA, Parton RG. Rab11, a small GTPase associated with both constitutive and regulated secretory pathways in PC12 cells. FEBS Lett. 1993; 334:175–182. [PubMed: 8224244]

Wittmann T, Waterman-Storer CM. Cell motility: can Rho GTPases and microtubules point the way? J Cell Sci. 2001; 114:3795–3803. [PubMed: 11719546]

Wu H, Rossi G, Brennwald P. The ghost in the machine: small GTPases as spatial regulators of exocytosis. Trends Cell Biol. 2008; 18:397–404. [PubMed: 18706813]

HIGHLIGHTS

- GEF-H1 functions in endocytic recycling and exocytosis.
- GEF-H1 activity regulates localization and assembly of the exocyst sub-complexes.
- Activation of RhoA by Ral GTPase that is dependent on GEF-H1 and Sec5 interaction.
- RhoA affects membrane traffic by regulating exocyst localization and assembly.

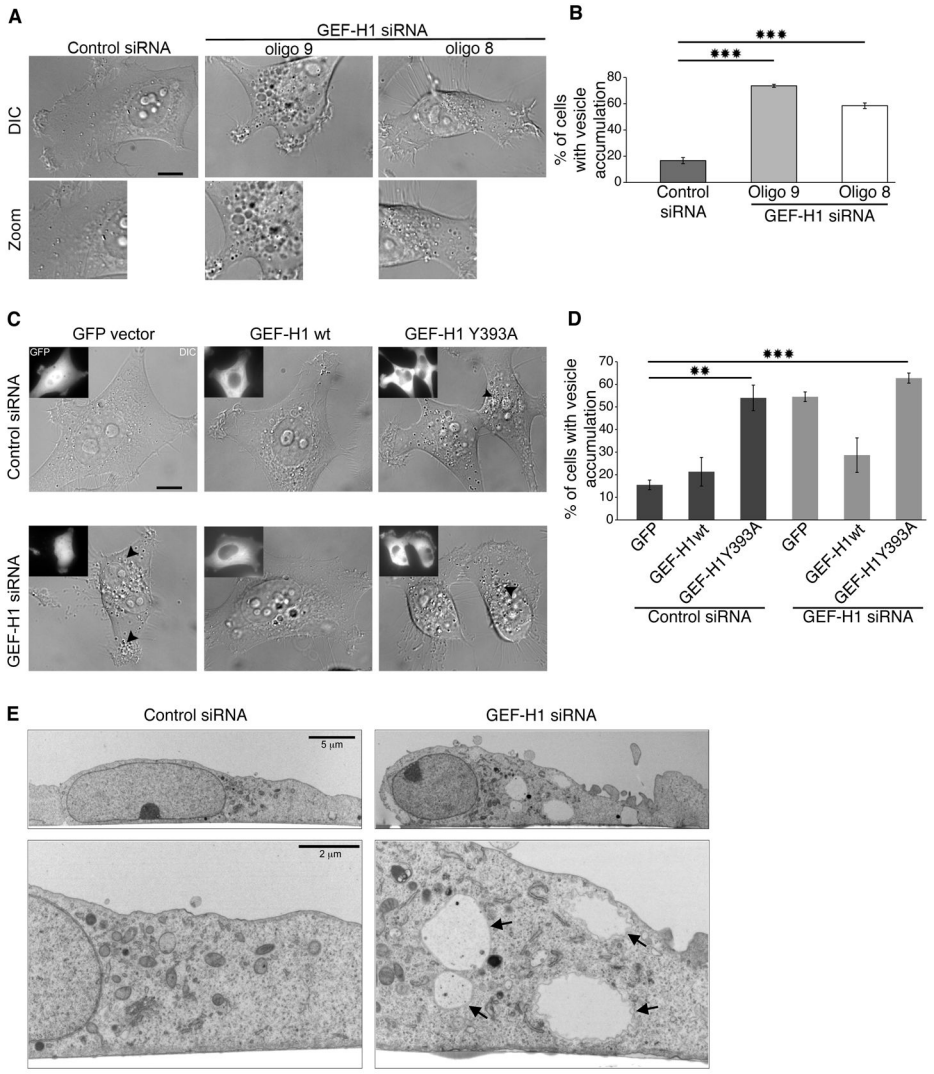

Figure 1. Perturbation of GEF-H1 function leads to accumulation of vesicular structures

(A)HeL a cells were transfected with either control siRNAor two different GEF -H1 specific oligonucleotide siRNA (#8 and #9). After 72 hrs, the cells were visualized using DIC. Scale bar, 10 μm. See also movies S1–3. (B) Percentage of cells showing accumulation of vesicles of varying sizes is shown for the control and GEF-H1-knockdown cells. Data represent means ± SD for approximately 80 cells/sample and results from three separate experiments are shown. Significance values were evaluated using two-tailed Student's t test ($^{***}p$ <0.0005). (C) Cells were transfected with GEF-H1 specific siRNA (oligo #9) to deplete the endogenous protein. After 48 hrs, depleted cells were transfected with siRNA resistant GEF-$H1^{wt}$or catalytically inactive mutant (GEF -$H1^{Y393A}$). Proteins were allowed to express for 20 hrs, and then cells were visualized under DIC (vesicles indicated by ▶). Scale bar, 10 μm. (D) The percentage of cells showing the accumulation of vesicles was calculated. More than 50 cells were analyzed for each sample. Data represent means ± SD from three independent experiments. Significance values were evaluated using two-tailed Student's t tests ($^{**}p< 0.005$; $^{***}p <0.0005$). (E) HeLa cells plated on plastic bottom dishes were transfected with control or GEF-H1 siRNA. 72hrs post -transfection, cells were processed using the Gilula *et al.* method and visualized using electron microscope(arrows represent vesicles). See also Figure S1 and Movies S1–3

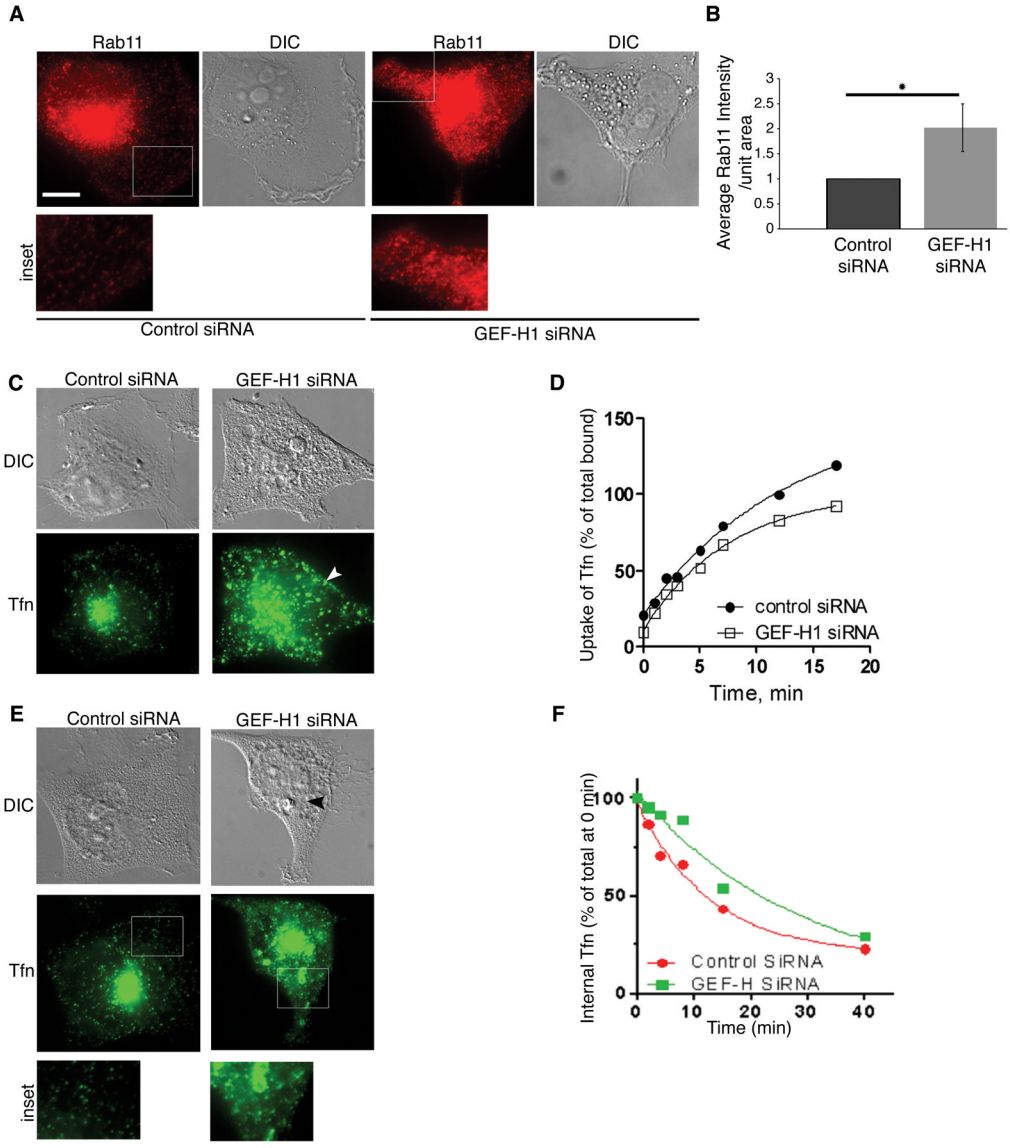

Figure 2. Depletion of GEF-H1 leads to accumulation of Rab11 positive vesicles and affects localization and recycling of Transferrin

(A) Control and GEF-H1-depleted cells were immunostained for Rab11. Cells were then visualized by fluorescence microscopy. Scale bar, 10 μm. (B) The fluorescence intensity associated with Rab11 outside the perinuclear endocytic recycling compartment was quantified and expressed relative to the control. > 60 cells were used to quantify the fluorescence intensity and results for three independent experiments are shown. Data represent means ± SD. Significance values were calculated using two-tailed Student's t test (*$p<0.05$).(C) Control and GEF-H1-depleted cells were incubated with Alexa 568 labeled transferrin for 10 min. Cells were then subjected to a brief acid wash to remove surface bound Tfn, fixed and visualized under fluorescence microscope. (D) Kinetics of Tfn uptake was measured for control and GEF-H1-depleted cells as described in methods. A representative plot, of four independent experiments is shown. (E) To study the effect of GEF-H1 depletion on Tfn recycling, the cells were incubated with labeled Tfn for 1 hr, this is the first time point (0 min). Most of the fluorescence in the control cells is associated with ERC and small endocytic vesicles. In GEF-H1-depleted cells besides localization to the

ERC a significant fraction was contained within large vesicles (marked by an ▶). (F) After washing out the labeled Tfn, cells were incubated with excess of unlabeled Tfn to enable recycling. Samples were taken out at different time points, subjected to acid wash, fixed and visualized by fluorescence microscopy. The fluorescence intensity associated with each cells was quantified and expressed as percentage of the intensity at time point 0 min. Representative graph from three different experiments is shown.

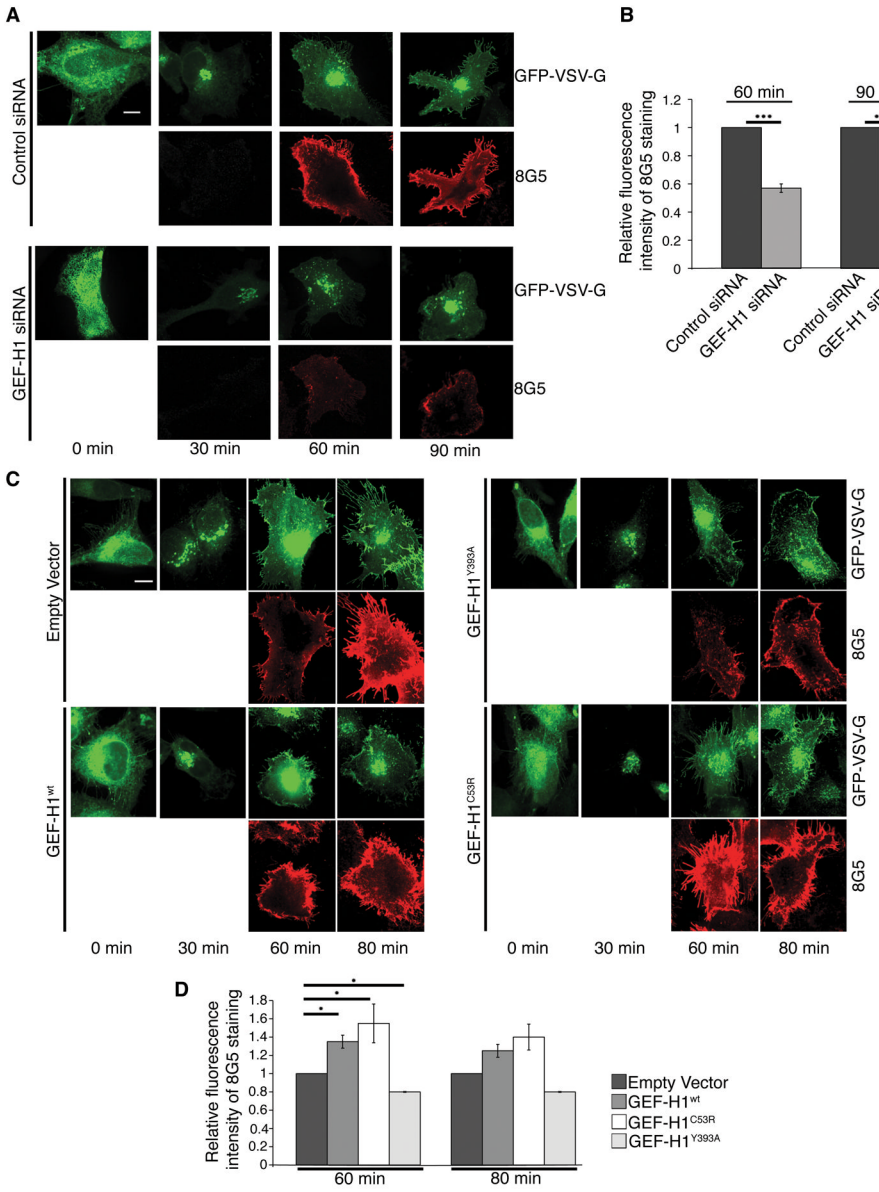

Figure 3. GEF-H1 is involved in exocytic trafficking of VSVG

(A) Cells were transfected with control or GEF-H1 specific siRNA. After 48 hrs, the cells were transfected again with GFP-VSV-G and immediately transferred to 40°C for 20 hrs. After removing the first sample (0 min), cells were shifted to 32°C. Samples were then taken at 30, 60 and 90 min post temperature shift, fixed, and immunostained with 8G5 antibody without permeabilization and observed using confocal microscope. Scale bar, 10 μm. (B)Fluorescence intensity associated with 8G5 staining of GEF-H1-depleted cells at time points 60 and 90 min was quantified and expressed relative to control cells. >80 cells were quantified for each sample and results of three independent experiments are plotted. Data represent means ± SD. Significance values were calculated using two-tailed Student's t test (***p <0.0005) (C) VSV-G trafficking assay was performed with cells co-transfected with GFP-VSV-G and empty vector, HA-GEF-H1^{wt}, GEF-H1^{Y393A} and GEF-H1^{C53R} as described earlier. Scale bar, 10 μm (D) Fluorescence intensity associated with 8G5 staining of the samples at time points 60 and 80 min was quantified and expressed relative to cells

transfected with empty vector. > 60 cells were quantified for each sample and results of three independent experiments are plotted. Data represent means ± SD. Significance values were calculated using two-tailed Student's t test (*$p<0.05$).

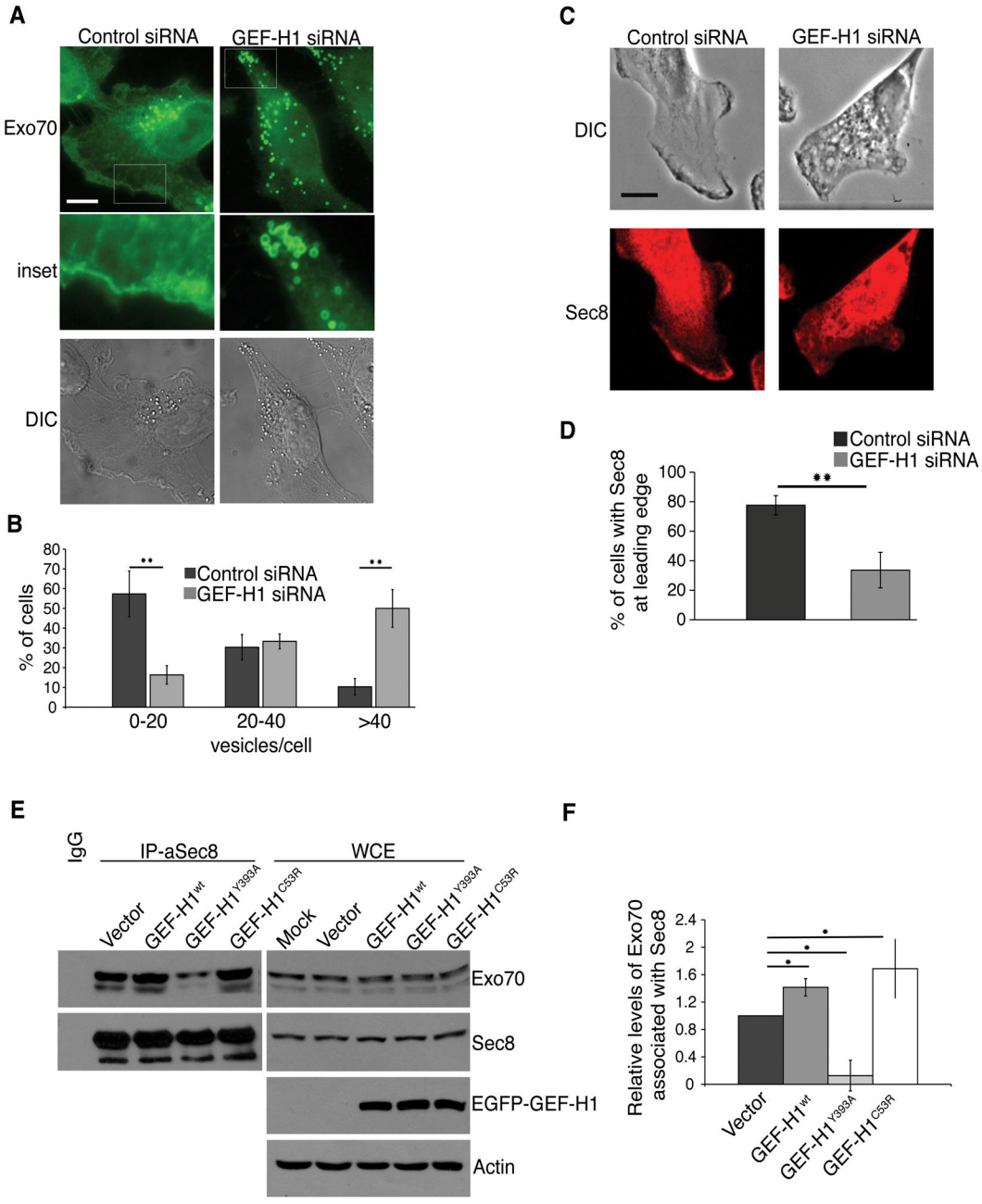

Figure 4. GEF-H1 depletion perturbs localization of exocyst component Exo70 and Sec8 as well as assembly/stability of exocyst complex

(A) Control and GEF-H1-depleted cells were immunostained for endogenous Exo70. The white boxes are enlarged in the bottom panel to show, in detail, features of Exo70 localization at/near the PM. Scale bar, 10 μm. (B) Number of Exo70-positive vesicles in control and GEF-H1-depleted cells were counted and the percentage of cells carrying indicated number of vesicles/cell were plotted. >50 cells were analyzed from three separate experiments. Data represent means ± SD. Significance values were calculated using two-tailed Student's t test ($^{**}p< 0.005$). (C) Immuno-staining of cells transfected with either control or GEF-H1 specific siRNA with α-Sec8 antibody. Scale bar, 10 μm. (D) Percentage of cells exhibiting leading edge localization of endogenous Sec8 in control and GEF-H1-

depleted cells was plotted. Data represent means ± SD. Significance values were calculated using two-tailed Student's t test (** $p<0.005$). (E) Lysates from cells transfected with empty vector, GEF-H1^{wt}, GEF-H1^{Y393A} or GEF-H1^{C53R} were subjected to immunoprecipitation (IP) with α-Sec8 antibody and the blots were then probed with α-Exo70 antibodies. The western blot against actin was used to show equal loading. (F)The band intensities were quantified using Image J software and the amount of Exo70 pulled-down from each sample was normalized to the levels of precipitated Sec8 and expressed relative to the sample transfected with empty vector. Data represent means ± SD. Significance values were calculated using two-tailed Student's t test (* $p<0.05$). See also Figure S2.

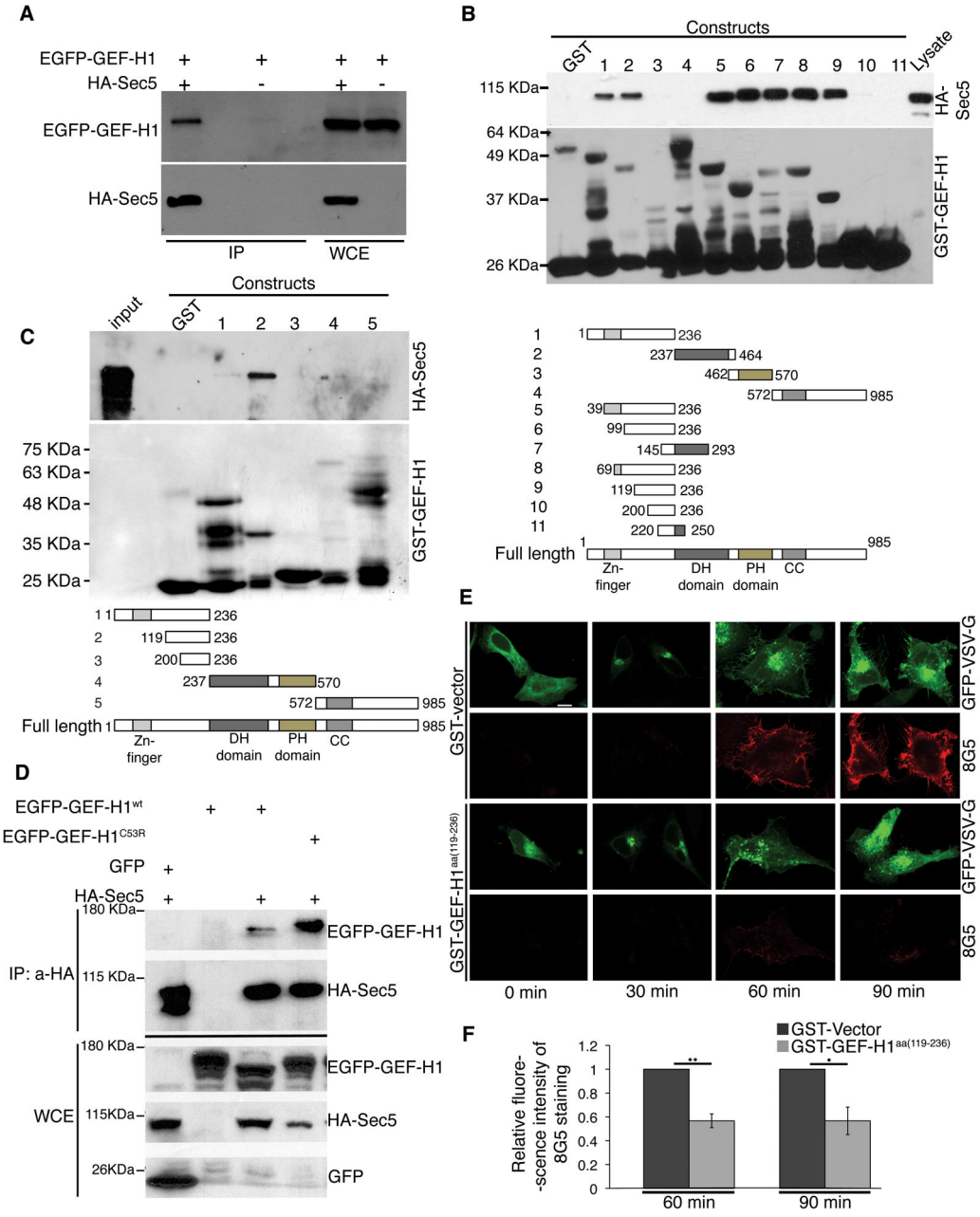

Figure 5. GEF-H1 interacts with exocyst protein Sec5

(A) EGFP-GEF-H1 and HA-Sec5 were co-expressed in HeLa cells. HA-Sec5 was then IPed using αHA antibody and probed for co-precipitation for EGFP-GEF-H1 by α-GFP antibody. (B) GST tagged truncation mutants of GEF-H1 (described in the bottom panel) were expressed in *E. coli* and purified using glutathione beads. The purified proteins were then used to pull-down Sec5 from lysates of cells expressing HA-Sec5. The pull-downs were analyzed with western blotting. (C) HA-Sec5 was *in vitro* translated using rabbit reticulocyte lysate system and added to recombinant GST or GST-GEF-H1 fragments described in the lower panel. Association between GST-GEF-H1 and HA-Sec5 was determined by pulling down GEF-H1 using glutathione beads and then probing for Sec5 using α-HA antibody. (D) HA-Sec5 was IPed from cell lysates co-expressing Sec5 and

GFP-GEF-H1^{wt} or constitutively active, microtubule binding-deficient mutant (GEF-H1^{C53R}), using α-HA antibody. Co-precipitation of GEF-H1 was analyzed using anti GFP antibody. (E) HeLa cells were co-transfected with GFP-VSV-G and GST-GEF-H1$^{(aa119-236)}$ or GST vector and the VSV-G assay was done as described earlier. Scale bar, 10 μm. (F) Fluorescence intensity associated with 8G5 staining of the samples at time points 60 and 90 min was quantified and expressed relative to that of the cells transfected with empty vector. >40 cells were quantified for each sample and results from three independent experiments are plotted. Data represent means ± SD. Significance values were calculated using two-tailed Student's t test (*$p<0.05$, **$p<0.005$). See also Figure S3.

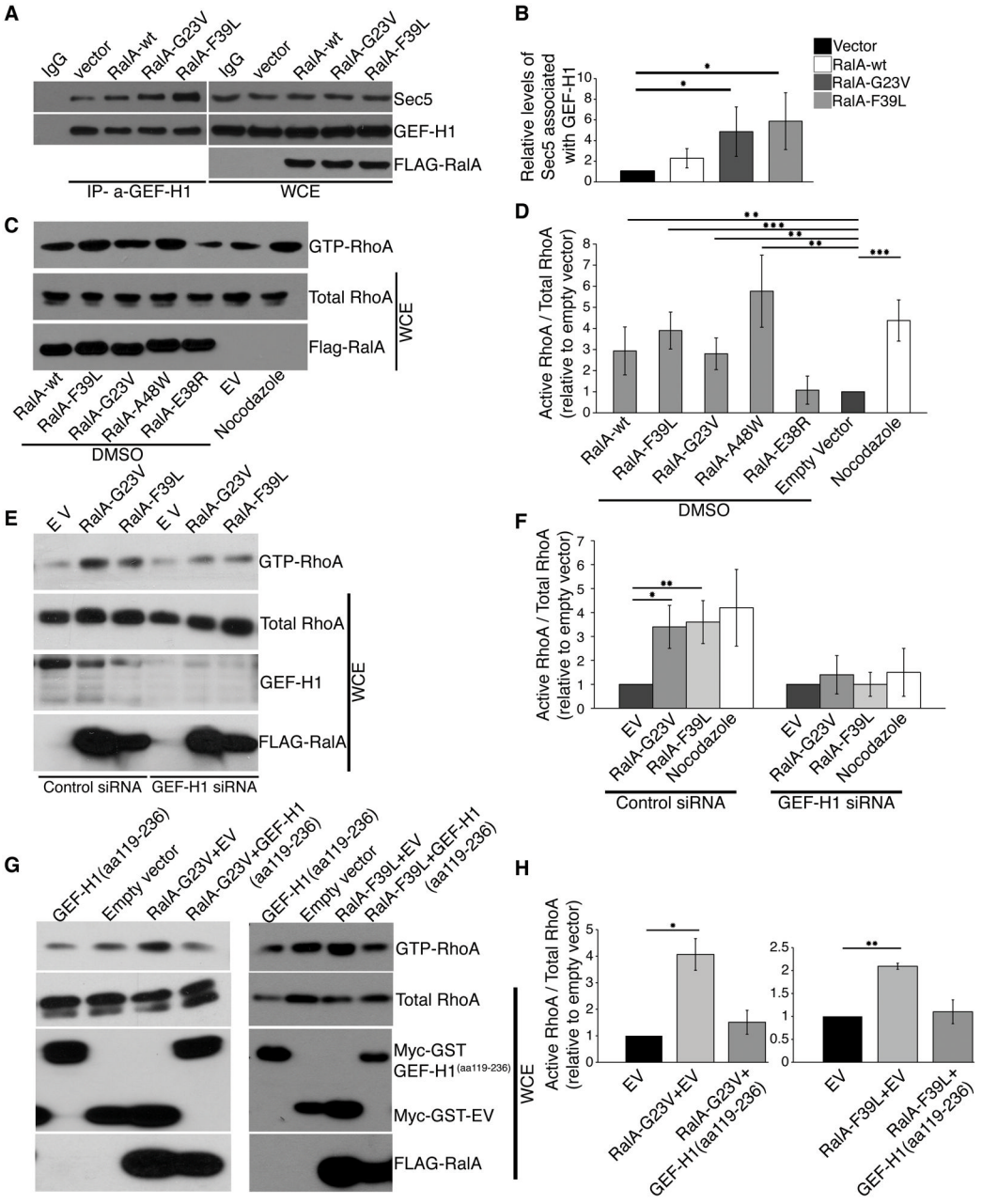

Figure 6. Ral GTPases regulate interaction between GEF-H1 and Sec5 and RhoA activation

(A) Endogenous GEF-H1 was IPed from HeLa cell lysates expressing empty vector, Flag-RalA^{wt}, constitutively active mutant RalA^{G23V} or fast-cycling active mutant RalA^{F39L}. (B) The band intensities were quantified and the amount of Sec5 pulled-down from each sample was normalized to the levels of immunoprecipitated GEF-H1 and expressed relative to the sample with empty vector. Data represent means ± SD. Significance values were calculated using two-tailed Student's t test (*$p<0.05$). (C) GTP-bound active Rho was pulled down from extracts of cells expressing empty vector (EV), RalA^{wt}, RaLA^{G23V}, RalA^{F39L}, Sec5 binding deficient mutant (E38R), and Exo84 binding deficient mutant (A48W), using Rhotekin-RBD beads (GST tagged Rhotekin-Rho binding domain). The blots were then probed for RhoA. (D) The band intensities of GTP-RhoA and total RhoA were quantified.

GTP-RhoA was normalized to the total RhoA levels in the lysates and expressed relative to the control cells with EV. Since enhanced RhoA activation has been reported in response to microtubule depolymerization, nocodazole treatment was used as a positive control (Chang et al., 2008). Results shown are average of four independent experiments. Data represent means ± SD. p values calculated by Student's t-test, $^{**}p< 0.005$, ***p<0.0005. (E) EV and active RalA mutants (G23V and F39L) were expressed in control and GEF-H1-depleted cells. Active RhoA was then pulled down from cell extracts using Rhotekin-RBD beads. The blots were probed with α-RhoA antibody. (F) RhoA activation induced by RalA in presence or absence of GEF-H1 was expressed as percentage of total RhoA in the lysate, and relative to the levels observed for control or GEF-H1depleted cells with EV, respectively (number of experiments=3; data represent means ± SD; *p<0.05, **p<0.005). (G) Lysates from cells transfected with indicated plasmids were used for RBD pull-down. (H) The band intensities of GTP-RhoA and total RhoA were quantified. Rho activation for cells expressing indicated proteins relative to the sample transfected with EV was calculated as described above (number of experiments=3; data represent means ± SD; p values; *p<0.05, **p<0.005).

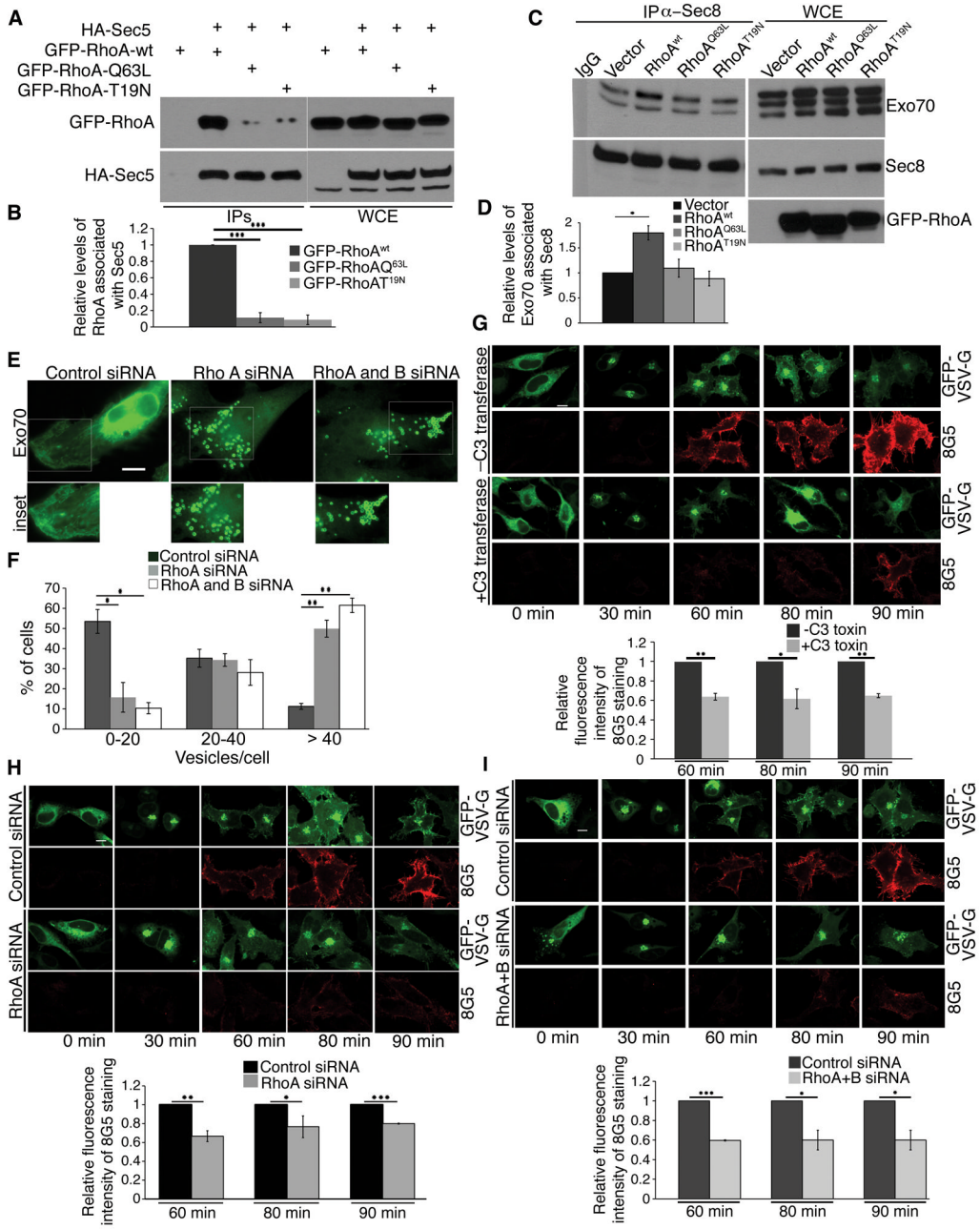

Figure 7. Rho GTPase regulates exocyst assembly/stability and localization

(A) Sec5 was IPed from cells expressing HA-Sec5 and either GFP-RhoA^{wt}, GFP-RhoA^{T19N}, or GFP-RhoA^{Q63L}. Co-IPof Rho proteins was detected by immunoblotting with α-GFP antibody. (B) The band intensities were quantified and the amount of RhoA associated with Sec5 was normalized to the levels of IPed Sec5. The fold change of interaction was expressed relative to the RhoA^{wt} sample. n=3; data represent means ± SD; ***p< 0.0005. (C) To analyze the effect of Rho mutants on interaction between Sec8 and Exo70 cells were transfected with EV the wild type, constitutively active (Q63L) or dominant negative (T19N) mutants. Sec8 was then IPed using α-Sec8 antibody from the lysates and co-IP with Exo70 was detected using α-Exo70 antibody. (D) The band intensities from the western blots were quantified and the amounts of Exo70 co-IPed were

normalized to the levels of Sec8 pulled down in respective samples. The fold change in interaction was expressed relative to the sample transfected with EV. Data represent means ± SD. Significance values were calculated using two-tailed Student's t test (*p<0.05). (E) Cells were transfected with control or RhoA and B specific siRNA oligonucleotides for 48 hrs. Cells were then fixed, immunostained with α-Exo70 antibody and visualized using fluorescence microscopy. Scale bar, 10 μm. (F) Number of Exo70-positive vesicles in control, RhoA-depleted, and RhoA and B co-depleted cells were counted and percentage of cells carrying the indicated number of vesicles/cell were plotted. >50 cells were analyzed from three separate experiments. Data represent means ± SD. Significance values were calculated using two-tailed Student's t test (*p<0.05, **p<0.005). (G) GFP-VSV-G-transfected HeLa cells were treated with cell permeable C3 transferase for 4 hrs before performing the trafficking assay. Quantification of the fluorescence intensity associated with 8G5 staining of the samples for time points 60, 80 and 90min was expressed relative to that of the untreated cells (no. cells > 40; data represent means ± SD; *p<0.05, **p<0.005). Scale bar, 10 μm. (H,I) HeLa cells were transfected with 20 nM of RhoA or RhoA+B specific siRNA oligonucleotides for 48 hrs. Then cells were transfected again with 20 nM of siRNA and GFP-VSV-G for 24 hrs. VSV-G trafficking assay was performed as described in methods. VSV-G insertion into the PM was assessed by staining the cells with 8G5 antibody and measuring the intensities at time points; 60, 80 and 90 min and expressing the values relative to that of the control siRNA transfected cells. > 50 cells were analyzed for each sample from three separate experiments. Data represent means ± SD. Significance values were calculated using two-tailed Student's t test (*p<0.05, **p<0.005, ***p< 0.0005). Scale bar =10μm. See also Figure S4 and Figure S5.